COPYRIGHT NOTICE

Optics Letters

In vivo time-gated diffuse correlation spectroscopy at quasi-null source-detector separation

M. Pagliazzi,[1,*] S. Konugolu Venkata Sekar,[2] L. Di Sieno,[2] L. Colombo,[1,2] T. Durduran,[1,3] D. Contini,[2] A. Torricelli,[2] A. Pifferi,[2,4] and A. Dalla Mora[2]

[1]ICFO—Institut de Ciències Fotòniques, The Barcelona Institute of Science and Technology, 08860 Castelldefels, Barcelona, Spain
[2]Politecnico di Milano, Dipartimento di Fisica, 20133 Milano, Italy
[3]Institució Catalana de Recerca i Estudis Avançats (ICREA), 08015 Barcelona, Spain
[4]Istituto di Fotonica e Nanotecnologie, Consiglio Nazionale delle Ricerche, 20133 Milano, Italy
*Corresponding author: marco.pagliazzi@icfo.es

Received 12 February 2018; revised 23 March 2018; accepted 7 April 2018; posted 18 April 2018 (Doc. ID 321030); published 16 May 2018

We demonstrate time domain diffuse correlation spectroscopy at quasi-null source-detector separation by using a fast time-gated single-photon avalanche diode without the need of time-tagging electronics. This approach allows for increased photon collection, simplified real-time instrumentation, and reduced probe dimensions. Depth discriminating, quasi-null distance measurement of blood flow in a human subject is presented. We envision the miniaturization and integration of matrices of optical sensors of increased spatial resolution and the enhancement of the contrast of local blood flow changes.

OCIS codes: (040.1345) Avalanche photodiodes (APDs); (170.5280) Photon migration; (170.6920) Time-resolved imaging; (170.3890) Medical optics instrumentation.

https://doi.org/10.1364/OL.43.002450

Time domain diffuse correlation spectroscopy (TD-DCS) is an optical, non-invasive technique that makes use of pulsed, but coherent, laser light to characterize the reduced scattering (μ_s') and absorption (μ_a) coefficients, and blood flow at a depth of a few centimeters [1,2]. TD-DCS was first proposed using short (ps) laser pulses and non-linear optical gating [3] which was not suitable for *in vivo* use. The demonstration of a viable system for TD-DCS on phantoms and small animals was recently provided by introducing narrow time gates that enabled the use of more compact laser sources and time-correlated single-photon detection [1]. The first *in vivo* TD-DCS blood flow measurements on humans were achieved using highly coherent, long (hundreds of picoseconds) Ti:sapphire pulses which enabled the use of broad gates [2].

The time-domain approach is beneficial since it increases the sensitivity of DCS to deep blood flow [4]. Depth discrimination, the ability to separate localized hemodynamic changes in deep tissue or layers from superficial ones, is achieved by selectively considering, in reflectance geometry, the photons with time-of-flight (TOF) within certain time gates of a few picoseconds [1] up to a few nanoseconds [2]. In this geometry, the use of a finite, non-null separation between the source and detector results in a decrease of photon detection rate at any gate [5]. Moreover, the source and detector optics distance of a few centimeters results in bulkier probes. This classic approach has the advantage of mainly detecting photons with long path lengths. The source-detector separation can be adjusted to alter the mean TOF. On the other hand, if the source-detector separation is reduced (practically to zero, i.e., null separation), short TOF photons are orders of magnitude more numerous than larger TOF ones [6,7]. As they carry information mainly from the shallowest layers of the probed tissue, they are usually not of interest, making them a nuisance since they could saturate most detectors and most time tagging electronics. Therefore, at null- and quasi-null separation, the selective gating of the long TOF, deep-reaching photons should be at the detector level [8]. If this is possible, the null- and quasi-null separation approaches provide various advantages in signal-to-noise, spatial resolution, and probe ergonomics [9]. The shape of sensitivity volume of the null separation has recently been reviewed in [10].

In this Letter, we show that we can achieve quasi-null separation TD-DCS using fast-gated SPADs (fgSPADs) that can be switched on and off in hundreds of picoseconds at every laser pulse period and acquire photons only during gates of a width of a few nanoseconds [10]. Then we use fgSPADs to recover the blood flow index (BFI) from the auto-correlation curves at a very short, ideally null, source-detector separation. We also report that, by using gated detectors, time-tagging electronics are not needed. In other words, common auto-correlators can be used to obtain TD-DCS curves in real time with a dramatic simplification of the detection electronics. This is an important step towards the realization of compact matrices of TD-DCS sensors.

Figure 1 shows our experimental setup. Briefly, we have used a custom-made, high temporal coherence pulsed Ti:sapphire laser operating in the active mode-locked regime (Fig. 1). The pulse repetition rate was 100 MHz, and the wavelength (λ) was 785 nm. We have split off a small fraction (<5%)

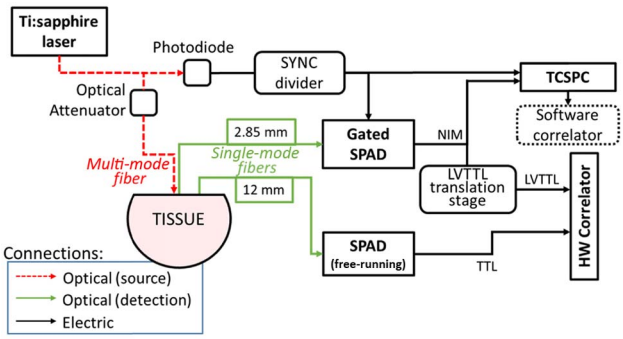

Fig. 1. Diagram of the experimental setup. The 12 mm source-detector separation detector is used as the standard to which the quasi-null separation TD-DCS is compared against.

of its light to a photodiode (OCF-401, Becker & Hickl, Germany) whose output generated the synchronization signal. Single-mode fibers (Neufern 780HP, 4.4 μm core diameter, cutoff wavelength 730 nm) were used for light collection. A SPAD detector (PDM, Micro Photon Devices, Italy) was used in a free-running (i.e., was not time gated) mode to carry out a standard DCS measurement at a source-detector separation (ρ) of 12 mm. This value was chosen to mimic our previous work [2]. Another SPAD, built in-house [11], was gated and synchronized with the photodiode signal. It was used to collect photons at short distances from the source. Since the maximum gating frequency allowed by this SPAD is 50 MHz, we have developed a fast circuit (SYNC divider) that reduces the number of synchronization pulses by accepting just one in two.

The arrival time of the photons was recorded by a time-correlated single photon counter (TCSPC) module (Pico Harp 300, PicoQuant, Berlin, Germany). A hardware (HW) correlator (Correlator.com, U.S.) computed the intensity auto-correlation curves of two independent channels every 2 s in real time.

The fgSPAD, nominally, has a 100 ps timing resolution and was connected to the TCSPC. For each detected event, the TCSPC recorded two time tags: the delay with respect to the laser synchronization signal and the overall (laboratory) arrival time with a coarser 20 ns timing resolution. A low voltage transistor-transistor logic (TTL) translation stage built using emitter coupler logic standard components was used to invert and amplify the nuclear instrumentation module output of the fgSPAD to make it compatible with one channel of the HW correlator. The TTL output of the free-running SPAD (coarser timing resolution, 250 ps) was connected directly to another channel of the HW correlator. The FoCuS-point software (SW) correlator [12] was modified and used in post-processing of the time-tagged data to compute the correlation curves with 2 s integration time.

The fgSPAD gate was open for 4 ns and synchronized with the laser pulse repetition frequency. The delay between the opening of the gate and the pulse emission (Δt_0) is by definition zero when it coincides with the peak of the laser pulse. In order to calibrate this, we have acquired an instrument response function (IRF) with the source and detector fibers facing each other, separated by a <0.2 mm thick diffuser and with a high attenuation of the source in order to avoid detector saturation.

The protocol was approved by the Ethical Committee of Politecnico di Milano and was conducted in agreement with the Declaration of Helsinki. The subject gave written consent before participation.

The probe was made of a black foam matrix. The detector fiber tips were separated by $\rho = 12$ mm (long separation) and $\rho = 2.85$ mm (quasi-null separation).

We have placed the probe gently on the brachioradialis muscle of a healthy subject (female, 26 years old). We have limited the laser power by using an optical attenuator to meet the maximum permissible exposure limit for human skin. We have estimated the superficial (skin and fat) thickness with a plicometer to be 13 mm. After 3 min of baseline measurement, the tourniquet, placed right below the shoulder joint, was inflated up to a pressure of 180 mmHg, well above the arterial pressure of the subject, and was released after 3 more minutes had passed.

We have fitted the electric field auto-correlation curves ($g_1(\tau)$, τ is the correlation delay time) to the model described in [2], evaluated numerically, given by the equation

$$g_1(\tau) = \int_{\Delta t_0}^{\infty} R(t) \exp(-k\tau t) \mathrm{d}t, \tag{1}$$

where $k = 2\mu_s' v k_0^2 \alpha D_B$, v is the speed of light in the medium (assumed constant), k_0^2 is the square of the wavenumber of light in the medium, αD_B is the BFI, D_B is effective Brownian diffusion coefficient of the moving scatterers, (i.e., red blood cells), and α is the ratio of moving to static scatters. $R(t)$ is the theoretical, time-resolved diffuse reflectance [13]. We note that Eq. (1) is not valid when photons that underwent only few scattering events are considered. The integration over the photon TOF (t) is carried out from $\Delta t_0 = 0$ for the ungated $\rho = 12$ mm case while, in the case of the quasi-null separation, Δt_0 was estimated prior to the cuff occlusion experiment by adjusting the fgSPAD delay while monitoring the TOF distribution (DTOF).

A separate time-resolved reflectance spectroscopy experiment with the same source and a free-running detector at 12 mm separation on the same location in the arm was used to measure the optical properties (μ_a and μ_s') that have been then used for computing $R(t)$ in Eq. (1). We have fitted the DTOFs at the large source-detector distance with a homogeneous model for photon diffusion with extrapolated boundary conditions [5], taking into account the measured IRF, and estimated the reduced scattering and absorption coefficients to be $\mu_s' = 10.3\ \mathrm{cm}^{-1}$ and $\mu_a = 0.14\ \mathrm{cm}^{-1}$.

In the IRF measurement configuration, we have set an initial, negative Δt_0, allowing the whole pulse to be resolvable within the gate [Fig. 2, orange line].

The effective width of the gate was measured to be 4 ns between the rising and falling edge at $1/10^4$ of the maximum intensity. We note that the imperfections at large TOFs after the closing of the gates are due to imperfections that are typical of fgSPAD [14] and are well below the signal level. The full width at half-maximum of the IRF was 350 ps. Given the performance of our system in terms of timing resolution, all the other contributions to the width of the IRF (for example, detector timing resolution, resolution of the timing electronics, and other less relevant effects) are negligible. We estimate that the laser pulse width is close to this value. We have then placed the probe on the arm, increased the delivered power to the maximum permissible exposure limit, and started recording the count rate at the detector. The time delay Δt_0 then was

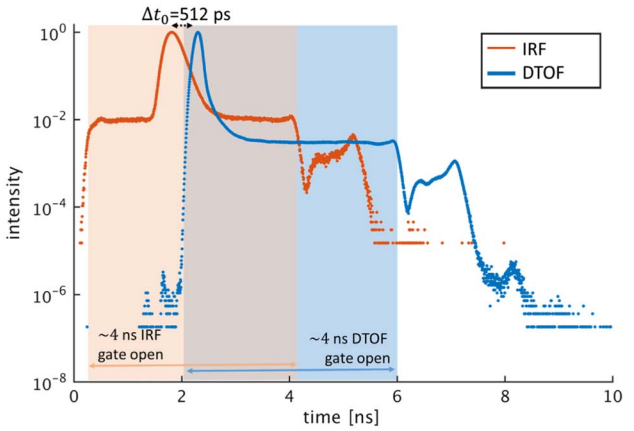

Fig. 2 IRF of the system (orange line) and a typical distribution of photon TOFs (DTOF, blue line) detected by the fgSPAD at quasi-null distance ($\rho = 2.85$ mm) on the arm during the baseline period.

increased in order to reject most of the photons that underwent shorter path lengths. The delay was finally set at $\Delta t_0 = 512$ ps [Fig. 2, blue line].

At the quasi-null separation, we have acquired 2.5×10^8 photons over 660 s at a mean count rate of 379 kHz, which is well within the limits of the fgSPAD, TCSPC, and HW correlator dynamic ranges. The tagged photon file saved by the TCSPC was 950 megabytes. We have acquired in parallel 318 intensity auto-correlation curves of 2 s integration time with the HW correlator for each channel. One of the eight channels correlated the signal detected by the fgSPAD at the quasi-null source-detector separation. Another channel processed the signal from the free-running SPAD at $\rho = 12$ mm with a mean count rate of 228 kHz. The data files to store the correlation of both channels occupied less than 3 megabytes in total. This demonstrates the efficiency of using a HW correlator, even for TD-DCS.

In Fig. 3, three representative auto-correlation curves from the gated detector at the quasi-null distance are reported from the baseline, occlusion, and hyperaemic peak (HE) periods. Two curves are shown for each measurement. In one case (continuous line), we have computed the auto-correlation from the time-tagged data acquired by the TCSPC by using the SW correlator while, in the other (dashed line), it has been computed by the HW correlator. The residual differences between the curves are compatible with the ~1 s precision of the synchronization between the acquisition time of the TCSPC and the HW correlator and the effect of experimental noise, showing the suitability of the HW correlator for TD-DCS.

In Fig. 4, we report the relative blood flow index (rBFI) normalized to the first 40 s (baseline, 100%) of the arm cuff experiment. The gray shaded area marks the duration of the arterial occlusion in the arm. The two lines represent measurements of the blood flow indices at the large (ungated, blue) and the quasi-null (gated, orange) source-detector separations. We have achieved a good signal-to-noise ratio and a two-second time resolution. The intercept of the intensity correlation curve (β) values averaged at 0.26 ± 0.03 for the gated quasi-null separation and at 0.21 ± 0.02 for the ungated long separation showing, once more, the benefit of the long-coherence, pulsed laser as detailed in [1,2]. The features of the baseline (0-180 s), occlusion (180 s-360 s), and the HE (360 s-420 s) are well evident and correspond to large differences in the rBFI, as expected from the literature [15].

Quantitatively, the estimated BFI dynamics at the quasi null source-detector separation is in good accordance, albeit, slightly noisier, with the measurement at $\rho = 12$ mm during most of the experiment. Furthermore, the quasi-null separation rBFI shows notably a ~37% higher HE during reperfusion, and a faster decay towards the baseline. This is expected since the gated, quasi-null separation measurement probes selectively deeper into the more metabolically active and reactive muscle tissue, as was observed in multi-distance measurements [15].

We note that we report our results for a very short source-detector separation of <3 mm. However, as previously demonstrated, there are no major differences between this very short ("quasi-null") and the ideally null distance [16,17]. Truly null source-detector separation is beyond the scope of this proof-of-principle experiment, but was demonstrated in the past for time-resolved experiments [8].

In summary, we have reported *in vivo* experiments from an adult volunteer using quasi-null separation TD-DCS, together

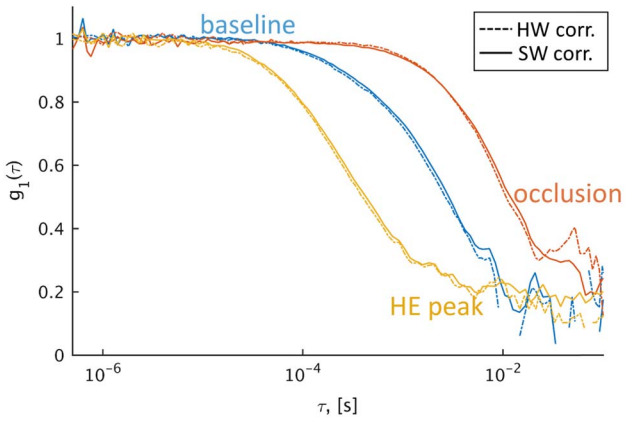

Fig. 3 Example auto-correlation (g_1) curves computed from the gated, quasi-null separation sensor from the HW (dashed line) and SW (solid line) correlators. Three periods are shown at the baseline (blue), the occlusion (red), and the HE (yellow).

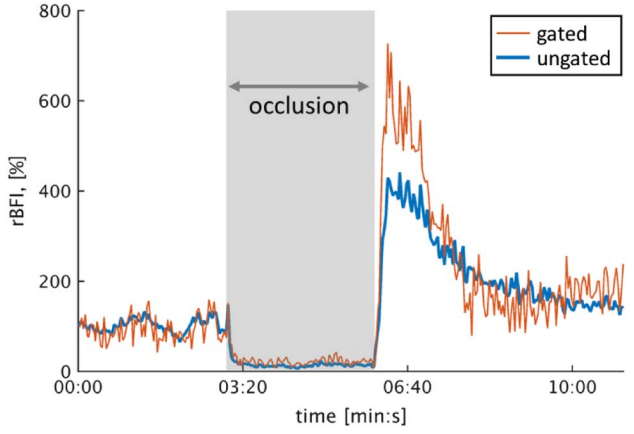

Fig. 4 rBFI during the arm cuff experiment, fitted from the HW correlator output. Two channels are represented, one for the gated, short separation detector (thin orange line), and one for the ungated, long separation detector (thick blue line).

with the feasibility of using a much simplified instrumentation on the detection side for TD-DCS. The usage of a common HW correlator does not require time tagging electronics, and the storage, as well as the processing, of large photon time-tagged files. In the future, the calculation of the blood flow can be embedded in the firmware of the HW correlators in real time. The reduction of the distance between the source and detector paves the way to integrated, miniaturized probe assemblies as few square millimeter patches on the tissue. In time-resolved spectroscopy applications, it has been demonstrated that the use of small, quasi-null source-detector distances allows an increase in the collection of photons and a higher contrast for the detection of localized changes [11,16]. We could now move towards achieving the same for DCS, with localized changes of blood flow, e.g., in the case of localized functional activation of the brain as suggested in [6].

Funding. Fundación Cellex; Instituto de Salud Carlos III (ISCIII) (DTS16/00087); Ministerio de Economía y Competitividad (MINECO) (DPI2015-64358-C2-1-R); "la Caixa" Foundation (LlumMedBcn); "Severo Ochoa" Programme for Centres of Excellence in R&D (SEV-2015-0522); Agència de Gestió d'Ajuts Universitaris i de Recerca (AGAUR) (2017 SGR 1380); Laserlab Europe IV; Horizon 2020 Framework Programme (H2020) (688303H2020-ICT-2015); Institució CERCA.

REFERENCES

1. J. Sutin, B. Zimmerman, D. Tyulmankov, D. Tamborini, C. W. Kuan, J. Selb, A. Gulinatti, I. Rech, A. Tosi, D. A. Boas, and M. A. Franceschini, Optica **3**, 1006 (2016).
2. M. Pagliazzi, S. Konugolu Venkata Sekar, L. Colombo, E. Martinenghi, J. Minnema, R. Erdmann, D. Contini, A. D. Mora, A. Torricelli, A. Pifferi, and T. Durduran, Biomed. Opt. Express **8**, 5311 (2017).
3. A. G. Yodh, P. D. Kaplan, and D. J. Pine, Phys. Rev. B **42**, 4744 (1990).
4. T. Durduran, R. Choe, W. B. Baker, and A. G. Yodh, Rep. Prog. Phys. **73**, 76701 (2010).
5. F. Martelli, T. Binzoni, A. Pifferi, L. Spinelli, A. Farina, and A. Torricelli, Sci. Rep. **6**, 27057 (2016).
6. A. Pifferi, A. Torricelli, L. Spinelli, D. Contini, R. Cubeddu, F. Martelli, G. Zaccanti, A. Tosi, A. Dalla Mora, F. Zappa, and S. Cova, Phys. Rev. Lett. **100**, 138101 (2008).
7. A. Puszka, L. Di Sieno, A. Dalla Mora, A. Pifferi, D. Contini, G. Boso, A. Tosi, L. Hervé, A. Planat-Chrétien, A. Koenig, and J.-M. Dinten, Biomed. Opt. Express **4**, 1351 (2013).
8. E. Alerstam, T. Svensson, S. Andersson-Engels, L. Spinelli, D. Contini, A. Dalla Mora, A. Tosi, F. Zappa, and A. Pifferi, Opt. Lett. **37**, 2877 (2012).
9. S. Saha, F. Lesage, and M. Sawan, in *IEEE International Symposium on Circuits and Systems (ISCAS)* (IEEE, 2016), pp. 333–336.
10. A. Pifferi, D. Contini, A. Dalla Mora, A. Farina, L. Spinelli, and A. Torricelli, J. Biomed. Opt. **21**, 91310 (2016).
11. L. Di Sieno, H. Wabnitz, A. Pifferi, M. Mazurenka, Y. Hoshi, A. Dalla Mora, D. Contini, G. Boso, W. Becker, F. Martelli, A. Tossi, and R. Macdonald, Rev. Sci. Instrum. **87**, 35118 (2016).
12. D. Waithe, M. P. Clausen, E. Sezgin, and C. Eggeling, Bioinformatics **32**, 958 (2015).
13. D. Contini, F. Martelli, and G. Zaccanti, Appl. Opt. **36**, 4587 (1997).
14. D. Contini, A. D. Mora, L. Spinelli, A. Farina, A. Torricelli, R. Cubeddu, F. Martelli, G. Zaccanti, A. Tosi, G. Boso, F. Zappa, and A. Pifferi, J. Phys. D **48**, 45401 (2015).
15. G. Yu, T. Durduran, G. Lech, C. Zhou, B. Chance, E. R. Mohler, and A. G. Yodh, J. Biomed. Opt. **10**, 24027 (2005).
16. L. Spinelli, F. Martelli, S. Del Bianco, A. Pifferi, A. Torricelli, R. Cubeddu, and G. Zaccanti, Phys. Rev. E **74**, 21919 (2006).
17. A. Torricelli, A. Pifferi, L. Spinelli, R. Cubeddu, F. Martelli, S. Del Bianco, and G. Zaccanti, Phys. Rev. Lett. **95**, 78101 (2005).